Turkish Journal of Electrical Engineering & Computer Sciences

http://journals.tubitak.gov.tr/elektrik/

Research Article

Turk J Elec Eng & Comp Sci
(2014) 22: 1130 – 1146

doi:10.3906/elk-1208-90

New approach using structure-based modeling for the simulation of real power/frequency dynamics in deregulated power systems

Mostafa EIDIANI[1], **Hossein ZEYNAL**[2,*]
[1]Khorasan Institute of Higher Education, Mashhad, Iran
[2]School of Engineering, KDU University College, Damansara Jaya, 47400 Petaling Jaya, Malaysia

Received: 29.08.2012 • **Accepted:** 08.01.2013 • **Published Online:** 15.08.2014 • **Printed:** 12.09.2014

Abstract: Load frequency control (LFC) is one of the significant ancillary services in the electricity markets. The major concerns with LFC models have long been their dynamic response and complexity, as well as market price sensitivity. To cater to the complexity of the dynamic model that is introduced by the LFC and algebraic constraints by the transmission network, the differential-algebraic equation is transformed into a set of ordinary differential equations. This is done by differentiating the network constraints under a certain assumption that can be held throughout the system. To make the model suitable in a market environment, the real power (MW) variable is substituted by the energy ($) variable to emphasize the price signal in the market. The obtained results show that the model is much easier to understand and simpler to implement. The computational complexity of the model is further reduced. Based on the performed simulations, the proposed LFC model functions better in a deregulated environment. A test case comprising 5 buses and 3 machines, with a 2-region system, is used to address the advantages of the proposed LFC model.

Key words: ODE, DAE, structural modeling, hierarchical control, LFC

1. Introduction

The restructuring in electric power systems is aimed at providing lower rates for end-use customers. This is achieved by running competitions among generators, while extirpating the monopolistic/oligopolistic aspects in transmission and distribution sectors [1]. As a result, various companies have emerged whose objective is exclusive and sometimes apposes others. This new business aspect impacts many technical problems in power systems [2].

With advent of deregulation in the electricity industry, load frequency control (LFC) has become more important in the decentralized operation of power systems [3,4]. Given as the most profitable ancillary services in deregulated power systems, the LFC attracts considerable attention from the system operators (SOs), as well as market players (MPs).

Each independent SO (ISO) is responsible for maintaining a seamless balance between the energy/load and frequency at every instance of the operation. This can be done by the precise coordination between the generator governor and LFC schemes to ensure that the system frequency will remain in the allowable region, as in [5] and [6].

There have been methods reported in the literature to improve the dynamic response of the LFC model

*Correspondence: hzeynal@gmail.com

in the market. In this sense, the LFC model in bilateral contracts was investigated extensively in [7,8]. These works tried to materialize their proposed model for practical use, but they were limited only to the bilateral transactions. Since the market type varies from country to country, this model would be unsuitable for universal use.

The optimal control technique proposed to model the LFC in the market in [9,10], turned out to be a complicated model with an excessive number of parameters involved. This model was somewhat cumbersome to be handled theoretically but presentations given by the authors promised practical use.

Artificial intelligence-based LFC models were also proposed in [11–15], which efficiently managed the nonlinearity and mathematically complexity of the classical was emerged by optimal control method. Although these efforts reduced some difficulties associated with classical methods, the resultant model was still huge enough to be applied in practice.

The robust decentralized LFC controller [16,17], based on the Riccati-equation approach and structured singular value (μ-synthesis), was developed while taking into account the uncertainties in a deregulated environment. Robust control techniques were used to tackle uncertainties existing in the deregulated power system. As a result, the stochastic nature in power markets is therefore accommodated in the model.

Furthermore, the LFC model can be formulated as a multiobjective optimization problem [18–21], which would be solved by the mixed $H2/H\infty$ control approach. However, this category of method has not found any broad application by MPs. Because this model creates a high order system of equations, it barely attracts the attention of the MPs.

An LFC-based bacterial foraging optimization algorithm (BFOA) was proposed in [22], suppressing oscillations in a deregulated power system. The BFOA is a heuristic-based optimization algorithm that has recently received great deal of attention due to its strong capabilities in solving complex real-world optimization problems. Although the evolved model can potentially be practical, further research is required to substantiate the model for more justifications.

A multiarea-based decentralized LFC model was later investigated in [23–26]. This model was based on characteristic matrix eigenvalues and the Lyapunov method. Since this method introduced a theoretically much simpler model, it has received much recognition from researchers as an appropriate LFC model. Based on the simulation results for a practical system, the controller ensures good performance, i.e. frequency deviation elimination, disturbance attenuation, and robustness under area load or frequency changes.

Considering all of the weaknesses of the conventional models explained previously, the complexity of the model structure, vague mathematical reasoning, and computational run-time, a structure-based LFC controller model is developed. It aims at improving the weaknesses in the traditional models that are described in the technical literature. In contrast to the model presented previously, the proposed model simplifies the system of equations by converting the original high-order differential-algebraic equation (DAE) problem into an equivalent low-order ordinary differential equation (ODE) system. In this sense, the accuracy of the problem remains the same for 2 systems of equations; however, the run time can significantly be shortened in the ODE-based model.

To better address the market characteristics of the LFC model, the power is translated to the energy price, which is denoted by the dollar ($) sign. This, however, enables the proposed model to respond to the changes in the system in a more market-induced sense than the traditional utility jargons. The reason is to resolve issues in the model presented in the literature related to the best use of the LFC model in a decentralized market.

In short, the real load/frequency controller mathematical model is improved. The DAE problem can be appropriately converted into an ODE problem. This is done by differentiating the network constraints under

the assumption that holds true for a wide range of system operations. Next, the power variable is replaced by the energy variable, emphasizing its importance in the market.

The main contributions of this work can be stated as:

1. Transforming the DAE equations into an equivalent ODE system of equations. This, however, alleviates most of computational burdens in the model.

2. Converting the variable associated to the real power change into an energy signal ($). This facilitates the model to be involved in a market-based environment

A test case comprising 5 buses and 3 machines, with a 2-region system, is used to address the efficiency of the proposed LFC model.

Furthermore, in contrast to the other models, the proposed structure-based LFC model offers many advantages. The model layout is easier to understand and implementable for practical use. In short, it results in a LFC controller that is less complex to be implemented in the real world by presenting a better dynamic response in a moderate amount of time.

2. Extended generic structure of the real power/frequency control scheme

The typical structure for real power/frequency control is shown in Figure 1. The governor control regulates the mechanical power applied to the generator shaft in order to stabilize the frequency [27,28].

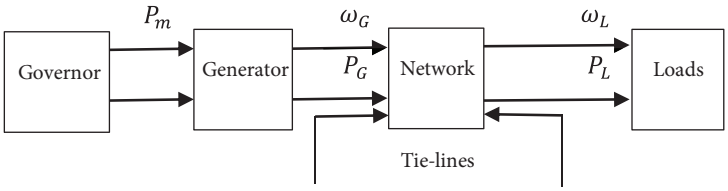

Figure 1. Real power/frequency control structure.

Let us reformulate the local dynamics of each generator machine, which can be expressed as [28]:

$$J_i\dot{\omega}_i = \tau_{m_i} - \tau_{e_i} - \tau_{d_i}, \qquad i = 1, .., m \tag{1}$$

where $\dot{\omega}_i$ is the rotating speed, or frequency, of the generator and J_i is the inertia of the rotating shaft. Symbols τ_{m_i}, τ_{e_i}, and τ_{d_i} represent the input mechanical torque, output electromagnetic torque, and mechanical damping torque, respectively.

Multiplying Eq. (1) by ω_i, one can get [28]:

$$M_i\dot{\omega}_i = P_{m_i} - P_{g_i} - P_{d_i} \tag{2}$$

Here, $M_i = J_i.\dot{\omega}_i$, P_{m_i}, P_{g_i}, and P_{d_i} are the input mechanical power, output electrical power, and mechanical damping power for ith generators, respectively. The damping power P_{d_i} is usually small and is assumed to be a linear function of the frequency $(P_{d_i} = D_i\omega_i)$, for which D_i is the damping coefficient.

Since the generator operates very close to the nominal frequency, one can typically take M_i as a constant. In the case of linear damping, Eq. (2) can be rewritten as [28]:

$$M_i.\dot{\omega}_i + D_i.\omega_i = P_{m_i} - P_{g_i} \tag{3}$$

Consider a simple governor–turbine–generator (G–T–G) set, shown in Figure 2. The governor regulates the valve opening P_{V_i} of the turbine, which in turn controls the mechanical power applied to the generator shaft P_{m_i}.

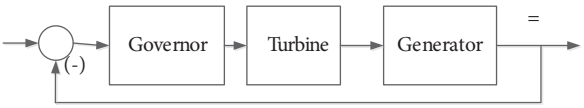

Figure 2. Primary control loop of a G–T–G set.

The turbine and the governor are modeled in general as a first-order system, given by [28]:

$$T_{u_i} \,.\, \dot{P}_{m_i} = -P_{m_i} + K_{t_i} P_{V_i} \tag{4}$$

$$T_{u_i} \,.\, \dot{P}_{m_i} = -P_{m_i} + K_{t_i} P_{V_i} \tag{5}$$

Here, T_{u_i} and T_{g_i} are the turbine and the governor time constants. Quantities T_{u_i}, T_{g_i}, K_{t_i}, and r_i are constant parameters. The frequency error signal is defined as $\omega_{err_i} = \omega_{ref_i} - \omega_i$, while ω_{ref_i} is the reference value for the governor.

The local state variables of the G–T–G set are defined as the frequency, mechanical power, and valve position, given by [29]:

$$X_{LC_i} = [\omega_i \quad P_{m_i} \quad P_{V_i}]^T \tag{6}$$

The superscript T reflects the transpose. The local dynamic model of the G–T–G set is described in a nonlinear state of space form [29]:

$$\dot{X}_{LC_i} = f_{LC_i}\left(X_{LC_i}, \omega_{ref_i}\right) - c_i P_{g_i} \tag{7}$$

where f_{LC_i} is the combination of Eqs. (3)–(5), and the vector c_i is given by:

$$c_i = \left[\begin{array}{ccc} \frac{1}{M_i} & 0 & 0 \end{array} \right]^T, \tag{8}$$

assuming that there exists a nominal operating point, which given by the equations: $x^0_{LC_i} = (\omega^0_i, P^0_{m_i}, P^0_{V_i})$ and $P_{g_i} = P^0_{g_i}$.

The linearized local dynamics in Eq. (7) can then be derived as:

$$\Delta \dot{x}_{LC_i} = A_{LC_i}.\Delta x_{LC_i} + b_i.\Delta \omega_{ref_i} - c_i.\Delta P_{g_i} \qquad i = 1, \ldots, m \tag{9}$$

where A_{LC_i} is the system matrix of local dynamics of each generator, and is given by [29,30]:

$$A_{LC_i} = \left[\begin{array}{ccc} \frac{-D_i}{M_i} & \frac{1}{M_i} & 0 \\ 0 & \frac{-1}{T_{u_i}} & \frac{K_{t_i}}{T_{u_i}} \\ \frac{-1}{T_{g_i}} & 0 & \frac{-r_i}{T_{g_i}} \end{array} \right] \tag{10}$$

and

$$b_i = \left[\begin{array}{ccc} 0 & 0 & \frac{1}{T_{g_i}} \end{array} \right]^T. \tag{11}$$

The frequency reference and generator output for the region in local state are as:

$$\Delta x_{LC} = \begin{bmatrix} \Delta x_{LC_1} \\ \vdots \\ \Delta x_{LC_m} \end{bmatrix}, \Delta\omega_{ref} = \begin{bmatrix} \Delta\omega_{ref_1} \\ \vdots \\ \Delta\omega_{ref_m} \end{bmatrix}, \quad \Delta P_g = \begin{bmatrix} \Delta P_{g_1} \\ \vdots \\ \Delta P_{g_m} \end{bmatrix}, \tag{12}$$

whereas the regional local system matrix can be given by:

$$A_{LC} = \begin{bmatrix} A_{LC_1} & & 0 \\ & \ddots & \\ 0 & & A_{LC_m} \end{bmatrix} = diag(A_{LC_1}, \cdots, A_{LC_m}) \tag{13}$$

and

$$b = \begin{bmatrix} b_1 & & 0 \\ & \ddots & \\ 0 & & b_m \end{bmatrix} = diag(b_1, \cdots, b_m), \tag{14}$$

$$c = \begin{bmatrix} c_1 & & 0 \\ & \ddots & \\ 0 & & c_m \end{bmatrix} = diag(c_1, \cdots, c_m). \tag{15}$$

The notation *diag(.)* stands for the diagonal matrix with each element of the vector as the diagonal element.

One obtains the local dynamic model for the entire region as:

$$\Delta\dot{x}_{LC} = A_{LC}.\Delta x_{LC} + b.\Delta\omega_{ref} - c.\Delta P_g \tag{16}$$

The above Eqs. (1)–(16) are the DAEs, which will be simplified to an ODE set of equations by the following assumptions, expressed in the next section.

2.1. Network coupling constraint modeling

Considering a system with a single region that contains m generators, the network constraints are typically expressed in terms of nodal-type equations. It requires a complex value of power, represented by S, to be equal to the both the value of the active and reactive powers; $S = P + jQ$ injected into each node:

$$S = diag\left(\hat{V}\right).Y^*_{bus}.\hat{V}^* \tag{17}$$

where $\hat{V} = Ve^{j\delta}$ is the vector of the nodal voltage, with magnitude V and phase δ, and Y_{bus} is the admittance matrix of the network. However, the focus is on the real power constraints. The real part of this equation, which is P, is extracted as:

$$P = Real\left(diag\left(\hat{V}\right).Y^*_{bus}.\hat{V}^*\right) = P\left(\delta, \hat{V}\right) \tag{18}$$

Let us define the vector of the real power flow from the neighboring areas into all of the generator nodes as:

$$F_g = \begin{bmatrix} F_{g_1} & \cdots & F_{g_m} \end{bmatrix}^T. \tag{19}$$

Furthermore, defining the vector of the real power flow from the neighboring areas into all of the load nodes as:

$$F_l = \begin{bmatrix} F_{l_1} & \cdots & F_{l_{n-m}} \end{bmatrix}^T, \tag{20}$$

emerges as:

$$P(\delta, \hat{V}) = \begin{bmatrix} P_g \\ -P_l \end{bmatrix} + \begin{bmatrix} F_g \\ F_l \end{bmatrix}. \tag{21}$$

In this expression, P_g is the generator power output and P_l is the real power consumed by the load.

To implement a structural model for an interconnected system, it is necessary to identify whether the power injected into the point is from the actual device or from the tie lines in the neighboring systems.

Based on the decoupling assumption ${}^{\partial P}/_{\partial V} = 0$, the linearized form of Eq. (18) can be obtained as:

$$\Delta F_g + \Delta P_g = J_{gg}\Delta\delta_g + J_{gl}\Delta\delta_l, \tag{22}$$

$$\Delta F_l - \Delta P_l = J_{lg}\Delta\delta_g + J_{ll}\Delta\delta_l, \tag{23}$$

where:

$$J_{ij} = \frac{\partial P_i}{\partial \delta_j}, \quad i, j = g, l, \tag{24}$$

$$\delta = \begin{bmatrix} \delta_g \\ \delta_l \end{bmatrix}. \tag{25}$$

Eqs. (24)–(25) are the elements of the Jacobian matrices evaluated at the given equilibrium operating point. It is obvious that DAE problems are more complex to handle than ODE problems.

Inversion of the Jacobian matrix in every real-world system is a big challenge. Assuming that, in the normal condition, J_{ll} should be invertible, then the sensitivity matrix can be referred to as:

$$C_\omega * -J_{ll}^{-1}.J_{1g} \tag{26}$$

The frequency deviation in load ω_l, in terms of frequency deviations in generator ω_g, and fluctuations in load power is expressed. Therefore, in accordance to Eq. (23), one can obtain:

$$\Delta\delta_l = C_\omega.\Delta\delta_g + J_{ll}^{-1}(\Delta F_l - \Delta P_l). \tag{27}$$

It can also be made by differentiating it with respect to time:

$$\Delta\omega_l = C_\omega.\Delta\omega_g + J_{ll}^{-1}(\Delta\dot{F}_l - \Delta\dot{P}_l). \tag{28}$$

In this equation, one can insert the below expression into Eq. (28):

$$\Delta\omega_g = \Delta\dot{\delta}_g = \begin{bmatrix} \Delta\omega_{g_1} & \cdots & \Delta\omega_{g_m} \end{bmatrix}^T. \tag{29}$$

After that, Eqs. (27) and (22) are combined, which results in:

$$\Delta P_g = K_p.\Delta\delta_g + D_p.\Delta P_l - \Delta F_e, \tag{30}$$

where:

$$K_p J_{gg} + J_{gl} C_\omega \tag{31}$$

$$D_p = -J_{gl}.J_{ll}^{-1}, \tag{32}$$

$$\Delta F_e = \Delta F_g + D_p.\Delta F_l. \tag{33}$$

Here, ΔF_e represents an effective tie line flow, which is seen by each generator; K_p reflects the effect of the generator frequency on the generator real power outputs; C_ω relates the generator frequency to the load frequency; and D_p is the different electrical distance of loads at different locations, as seen by the generators.

Let us differentiate with respect to time on both sides of Eq. (30), which results in:

$$\Delta\dot{P}_g = K_p.\Delta\omega_g + D_p.\Delta\dot{P}_l - \Delta\dot{F}_e. \tag{34}$$

This equation defines the relation among all of the generator's real power outputs, the tie line flows into the system, and the load variations through the network characteristics are specified by 2 important matrices, K_p and D_p. Detailed studies on these matrices are presented in the next sections.

2.2. The state space characterization

The generator frequency is part of the local generator state, which can be denoted by:

$$\omega_g = H.x_{LC}, \tag{35}$$

whereas:

$$H \propto diag\,(h, \ldots) \tag{36}$$

Next, by combining Eqs. (34) and (16), one can get:

$$\begin{bmatrix} \Delta\dot{x}_{LC} \\ \Delta\dot{P}_g \end{bmatrix} = \begin{bmatrix} A_{LC} & -c \\ K_p.H & 0 \end{bmatrix} \begin{bmatrix} \Delta x_{LC} \\ \Delta P_g \end{bmatrix} - \begin{bmatrix} -b.\Delta\omega_{ref} \\ \Delta\dot{F}_e \end{bmatrix} + \begin{bmatrix} 0 \\ D_p \end{bmatrix} \Delta\dot{P}_l \tag{37}$$

This equation shows the linearized model of standard state space, including a single region in the interconnected system. It represented in terms of the tie line flows with m generators and n nodes.

3. Converting power (MW) to the energy ($) variable

To further extend the application of the LFC in the market, additional amendments are required to be applied to the formulation. It can be shown that the angle, power, valve, and other variables are not efficient to model in the new environment. In contrast to other variables, the energy variable is the main parameter, which can be converted into the price. Therefore, the real power generation variable is replaced by the energy price. Similarly, the power consumption is converted to the energy consumption variable. Hence, the fresh state space can then be characterized by:

$$\Delta E_{g_i} = \int \Delta P_{g_i}.dt \;\; \Rightarrow \;\; \Delta\dot{E}_{g_i} = \Delta P_{g_i}, \tag{38}$$

$$\Delta E_{l_i} = \int \Delta P_{l_i}.dt \quad \Rightarrow \Delta \dot{E}_{l_i} = \Delta P_{l_i}, \tag{39}$$

where ΔE_{g_i} and ΔE_{l_i} are the generator energy generation and load energy consumption.

Next, we combine Eq. (38) with Eq. (30), resulting in:

$$\Delta \dot{E}_{g_i} = K_p.\Delta\delta_g + D_p.\Delta \dot{E}_{l_i} - \Delta F_e. \tag{40}$$

If one performs the integration with respect to time over Eq. (3), and linearizes it, then:

$$M_i.\Delta\dot{\delta}_i + D_i.\Delta\delta_i = \int \Delta P_{m_i}.dt - \Delta E_{g_i}. \tag{41}$$

Performing integration on Eqs. (4) and (5), and then linearizing them:

$$(4) \Rightarrow \quad T_{u_i}.\Delta P_{m_i} = -\int \Delta P_{m_i}.dt + K_{t_i}.\int \Delta P_{V_i}.dt \tag{42}$$

$$(5) \Rightarrow \quad T_{g_i}.\Delta P_{V_i} = \int \Delta\omega_{err_i} dt - r_i.\int \Delta P_{V_i}.dt \tag{43}$$

To simplify Eqs. (42) and (43), it is assumed that $\Delta\omega_{ref_i} = 0$, and $\Delta\omega_{err_i} = \Delta\omega_{ref_i} - \Delta\omega_i$, which then leads to $\Delta\omega_{err_i} = -\Delta\omega_i = -\Delta\dot{\delta}_i$, thus:

$$\int \Delta P_{m_i}.dt = -T_{u_i}.\Delta P_{m_i} - K_{t_i}(\frac{T_{g_i}}{r_i}\Delta P_{V_i} + \frac{\Delta\delta_i}{r_i}). \tag{44}$$

Combining Eqs. (44) and (41) gives:

$$M_i.\Delta\dot{\delta}_i + D_i.\Delta\delta_i = -T_{u_i}.\Delta P_{m_i} - K_{t_i}(\frac{T_{g_i}}{r_i}\Delta P_{V_i} + \frac{\Delta\delta_i}{r_i}) - \Delta E_{g_i}. \tag{45}$$

To further simplify the DAE equations, another assumption can be made. Let us add δ_i from Eq. (45) to Eqs. (4) and (5), and then linearize it with the assumption that holds $\Delta\omega_{err_i} = -\Delta\omega_i = -\Delta\dot{\delta}_i$, therefore:

$$\Delta\dot{P}_{m_i} = \frac{-1}{T_{u_i}}\Delta P_{m_i} + \frac{K_{t_i}}{T_{u_i}}\Delta P_{V_i}, \tag{46}$$

$$\Delta\dot{P}_{V_i} = \frac{D_i.\Delta\delta_i + T_{u_i}.\Delta P_{m_i} + \frac{K_{t_i}}{r_i}(T_{g_i}\Delta P_{V_i} + \Delta\delta_i) + \Delta E_{g_i}}{M_i.T_{g_i}} \frac{-r_i.\Delta P_{V_i}}{T_{g_i}}. \tag{47}$$

Consequently, the local state variables can be defined as $x_{N_i} = \begin{bmatrix} \delta_i & P_{m_i} & P_{V_i} \end{bmatrix}^T$. However, to develop the local dynamics for all of the generator units in the region, one can combine Eqs. (45)–(47), which leads to:

$$\Delta\dot{x}_{N_i} = A_{N_i}.\Delta x_{N_i} - c_{N_i}.\Delta E_{g_i}, \tag{48}$$

in which:

$$c_{N_i} = \begin{bmatrix} \frac{1}{M_i} & 0 & \frac{-1}{M_i.T_{g_i}} \end{bmatrix}^T \tag{49}$$

and

$$A_{N_i} = \begin{bmatrix} \frac{-D_i}{M_i} - \frac{K_{t_i}}{M_i.r_i} & \frac{-T_{u_i}}{M_i} & \frac{-K_{t_i}.T_{g_i}}{M_i.r_i} \\ 0 & \frac{-1}{T_{u_i}} & \frac{K_{t_i}}{T_{u_i}} \\ \frac{D_i.r_i+K_{t_i}}{M_i.T_{g_i}.r_i} & \frac{T_{u_i}}{M_i.T_{g_i}} & \frac{K_{t_i}}{M_i.r_i} - \frac{r_i}{T_{g_i}} \end{bmatrix}. \tag{50}$$

Similar to Eqs. (12)–(16), considering any single region with (m) generators, then:

$$\Delta\dot{x}_N = A_N.\Delta x_N - c_N.\Delta E_g. \tag{51}$$

After that, imitating the same trajectory explained for Eq. (35) gives:

$$\delta_g = H.x_N. \tag{52}$$

This will require combining Eqs. (51) and (40), and, as a result, the new state space model forms as:

$$\begin{bmatrix} \Delta\dot{x}_N \\ \Delta\dot{E}_{g_i} \end{bmatrix} = \begin{bmatrix} A_N & -c_N \\ K_p.H & 0 \end{bmatrix} \begin{bmatrix} \Delta x_N \\ \Delta E_g \end{bmatrix} - \begin{bmatrix} 0 \\ \Delta F_e \end{bmatrix} + \begin{bmatrix} 0 \\ D_p \end{bmatrix} \Delta\dot{E}_l \tag{53}$$

This equation is the new state space model that is efficient for new systems and can practically be substituted instead of the model portrayed in Eq. (37). For further reading, the secondary control scheme is given in Appendix I.

4. Numerical simulation and discussion

A 5-bus power system is chosen to illustrate the proposed model. A single-line diagram of the example is shown in Figure 3.

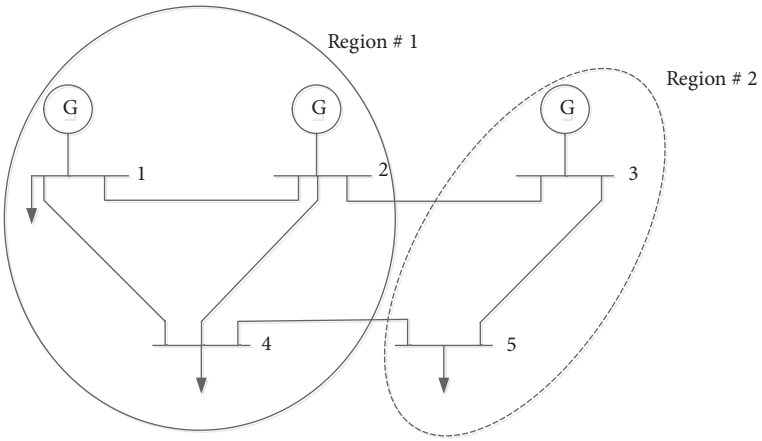

Figure 3. Illustrative 5-bus system.

To emphasize the deregulated environment and competitive market definition, this test case is formed as a 2-region system. On the other hand, region (I) consists of generator companies (GENCOs) located at buses 1 and 2, while a distribution company (DISCO) is located at bus 4. In contract to GENCOs, which are paid based on the market clearing price (MCP), DISCOs pay to buy energy at the MCP.

Similarly, region (II) comprises a GENCO that sells power at bus 3 and a DISCO in bus 5. There are 2 tie lines connecting GENCOs 2 and 3, and the DISCOs at bus 4 to bus 5. The data used in the simulation are listed in Table 1.

Table 1. Per-unit data for the 5-bus example.

PARAMETER	GEN 1	GEN 2	GEN 3
M	10	5	3
T_u	0.2	0.2	0.2
r	19	19	19
K_t	0.107	0.107	0.107
T_g	0.25	0.25	0.25
D	0.5	0.4	0.4

Line parameters

B	G	FROM	TO
10	1	2	1
10	1	4	1
10	1	4	2
10	1	5	3
0.5	0.05	3	2
0.5	0.05	5	4

Load flow data

BUSES 1, 2, AND 3 ARE VOLTAGE CONTROL (1)
Load bus 1 = 0.5722 + j 0
Load bus 4 = 1.2 + j 0.2
Load bus 5 = 1.2 + j 0.3

All of the simulations are done using MATLAB software. The K_p matrix and eigenvalues are calculated and given as:

$$K_p = \begin{bmatrix} 15.0074 & -14.7883 & -0.2190 \\ -14.8349 & 15.5537 & -0.7188 \\ -0.2106 & -0.6892 & 0.8998 \end{bmatrix}.$$

In this system, the eigenvalues are: –0.0364 ± j2.1338, –0.0622 ± j0.5943, and –75.99.

The elaborated numerical state-space matrix of the problem is given in Appendix II. Moreover, the controllability and observability of such a problem is demonstrated in Appendix III.

Figure 4 depicts the reaction of the participants in the market when the LFC model is used. It represents the DISCO 4 reaction when the price of energy changes in the market. It shows that the DISCO 4 consumption values follow the changes in the price of the deliverable energy.

Figures 5 and 6 depict the response of the consumption variation at bus 4. In Figures 5 and 6, P_g indicates the change in the conventional model, whereas E_g represents the reflection of such a change in the load of the proposed LFC model. In addition, Figure 5 also provides the energy difference in the proposed model.

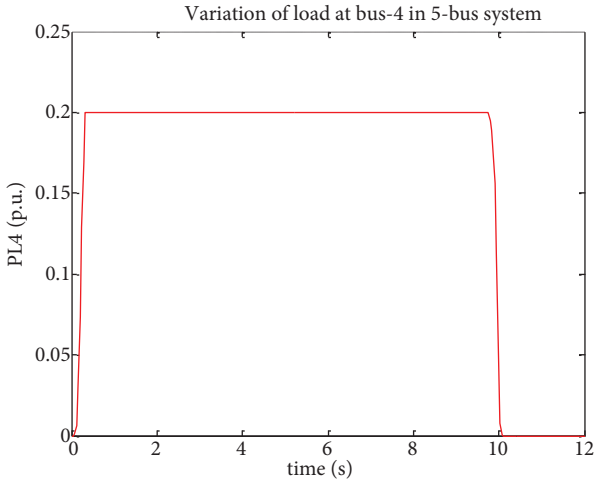

Figure 4. Load variation at bus 4.

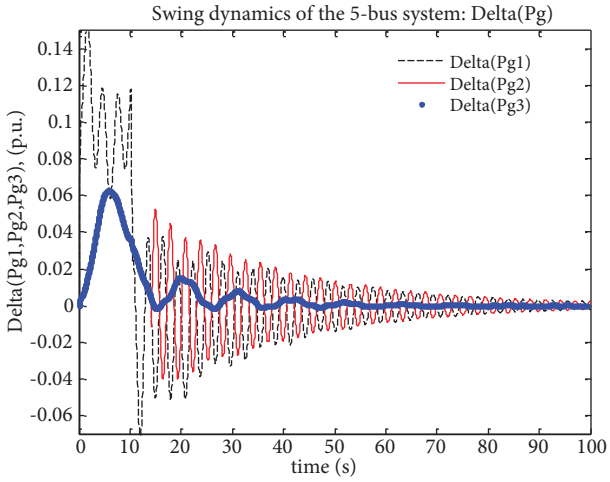

Figure 5. Response of the old system to the load variation at bus 4 (swing dynamics of the 5-bus example (P_g) and the energy differentiation of the new system to the variation at bus 4).

According to Figure 5, the fast and slow oscillation areas highlight the previously calculated eigenvalues.

In contrast to the conventional model, Figures 7 and 8 demonstrate the response of the proposed LFC model subject to the variation at DISCO 4 when the price is soaring in the market. This response, however, is similar to the situation when a FACTS device is used in direct tie line control.

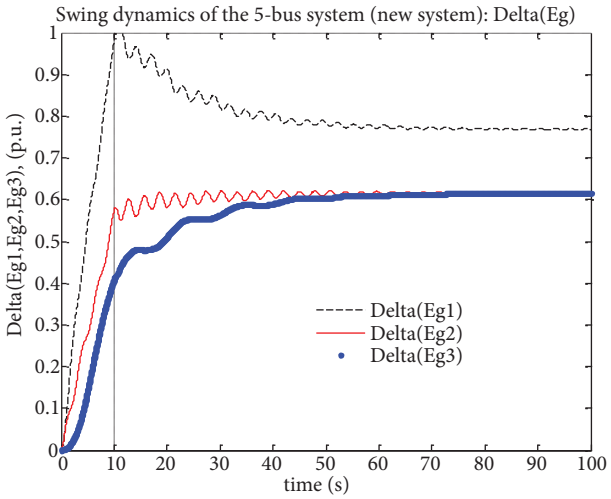

Figure 6. Response of the new system to the variation at bus 4 (swing dynamics of the 5-bus example (E_g)).

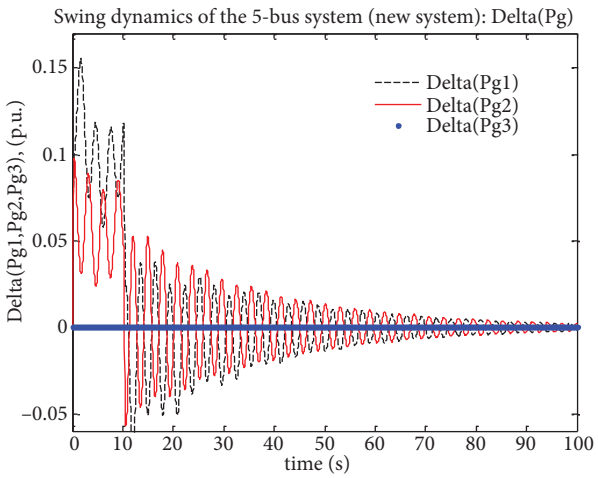

Figure 7. Response of the new system to the load variation at bus 4 with the nonresponse from generator 3 (P_g).

The energy oscillations always follow price fluctuations in the market to emphasize the higher profits that sellers can earn and how the buyers can save. In fact, it has been one of the virtues with the proposed model that makes it more efficient to be applied in a deregulated environment. This is because the energy variable procures a better reaction for the MPs than other variables. This is to make the LFC model as price-responsive as the MW-change.

As far as the energy price is concerned, one could always recast the formulation, for example, the DISCO 5 consumption amount subject to any change in GENCO 3 can simply be expressed by $P_{L5} = -E_{g3}$.

However, Figures 9 and 10 show the response in the proposed model when the variation of DISCO 4 is affected by the energy sold (change of the power injection in the bus) at GENCO 3. Figure 11 visualizes the variation at DISCO 5. These oscillations result in the system cost being at the minimum expense. The same trajectory is performed for the other DISCOs.

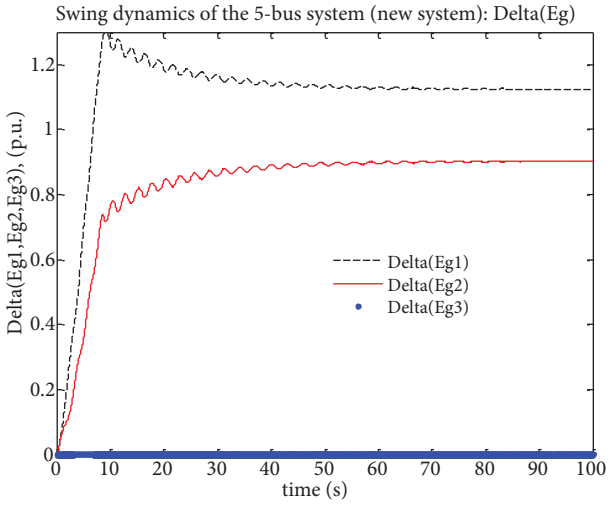

Figure 8. Response of the new system to the variation at bus 4 with the nonresponse from generator 3 (E_g).

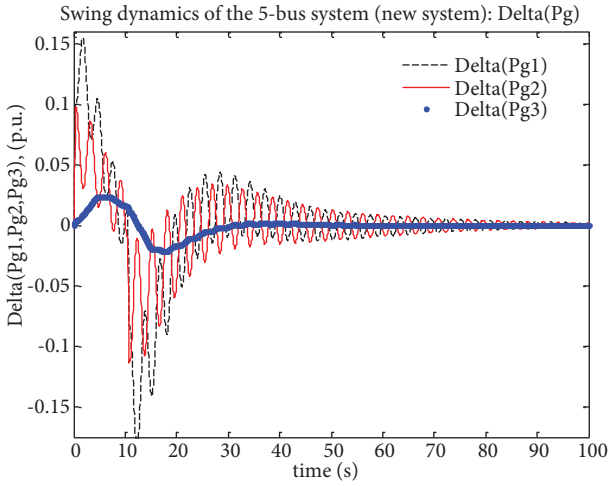

Figure 9. Response of the new system to the variation at bus 4 with the variation at bus 5 (P_g).

Based on the obtained simulation results and Figures 10 and 11, which are represented for the response of the proposed model, one can observe that this model outperforms the conventional model. However, one can infer by comparing Figure 5 with the results shown in Figures 10 and 11.

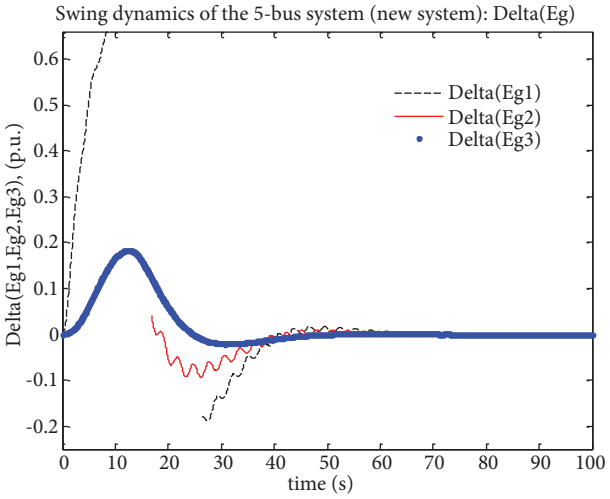

Figure 10. Response of the new system to the variation at bus 4 with the variation at bus 5 (E_g).

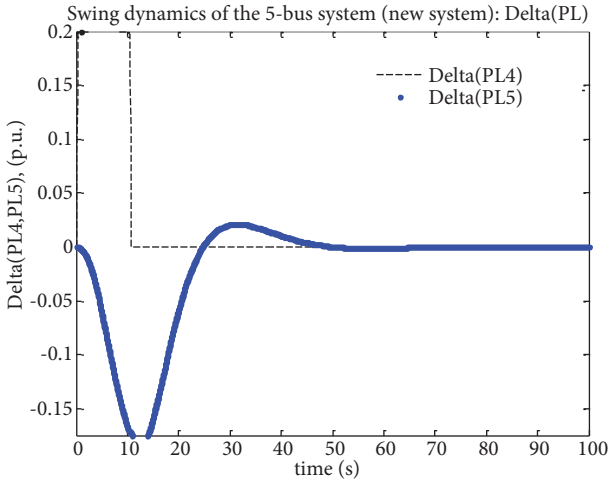

Figure 11. Response of the variation at bus 5 subject to the variation at bus 4.

The proposed LFC model is more suitable to be utilized in deregulated systems. In all of these experiments for any GENCO or DISCO, the price signal condition in the market turns out to be a key issue for further change and it is given in the horizontal axis.

Table 2 presents a comparison of 2 LFC models, for which one is based on a DAE and another uses an equivalent ODE equation system. This, however, is one of the computational advantages of the proposed LFC model. It is conceptually straightforward to explain that when one converts high-order equations to low-order ones, as in the ODE-based model, the solution results in a reduced execution time. Nevertheless, Table 2 itself shows the speed-up improvement percentages of the ODE-based model over the traditionally used DAE model.

Table 2. Comparison of the DAE-based model and ODE-based model.

G-T-G set parameters

DAE (s)	ODE (s)	Percent increase
0.04185	0.035586.	17.6
0.04157	0.033474	24.2
0.034432	0.030232	13.9
0.03458	0.029081	18.9
0.03791	0.031914	18.8
0.04042	0.035017	15.5
Mean: 0.03785	Mean: 0.03255	Mean: 18.2

5. Conclusion

In this paper, an improved dynamic model for real power/frequency control in a deregulated environment is developed. A conversion from a DAE system of equation to an equivalent ODE formulation is done using 2 sets of assumptions. First, a fast decoupled load flow is used to cater to the Jacobian matrix inversion. Second, a linearization process enforces the resultant DAE (Eqs. (45)–(50)). As such, the model becomes computationally efficient for practical use. Furthermore, to make the model suitable for competitive markets, the power variable is replaced by the energy variable, emphasizing the price signal over the MW change in the system. Based on the simulation results, the proposed model offers a less complex equation system compared with previous works reported that employed an ODE. The improved LFC mathematical model is easier to understand and implement. The obtained results exhibit that the dynamic response of the improved LFC model is well-functioning for small changes in the system frequency. The improved LFC model would be a much more suitable choice as a market participant to achieve the objectives, as the proposed model provides a price-oriented reaction mechanism, rather than the real-power indices that were applied in previous LFC models in the technical literature.

A. Appendix: Secondary control scheme

In this section, a simple discrete-time dynamic model over a secondary time scale is derived. The purpose of regulation at the regional secondary level is to update the frequency reference value for each participating G–T–G set over the discrete time instant $k.T_s$. Therefore, steady-state frequency errors are eliminated. The discrete-time actions of the updating frequency reference values result in a discrete event process in frequencies on the secondary level.

In primary control, to simplify Eqs. (42) and (43), it is assumed that $\Delta\omega_{ref_i} = 0$, but in secondary control, one may have: $\Delta\omega_{ref_i} \neq 0$ and $\Delta\omega_{err_i} = \Delta\omega_{ref_i} - \Delta\omega_i$, which leads to $\Delta\omega_{err_i} = \Delta\dot{\delta}_{ref_i} - \Delta\dot{\delta}_i$; thus

Eq. (44) is rewritten as:

$$\int \Delta P_{m_i}.dt = -T_{u_i}.\Delta P_{m_i} - K_{t_i}(\frac{T_{g_i}}{r_i}\Delta P_{V_i} + \frac{\Delta\delta_i + \Delta\delta_{ref_i}}{r_i}) \tag{A.1}$$

Combining Eqs. (A.1) and (41) gives:

$$M_i.\Delta\dot{\delta}_i + D_i.\Delta\delta_i = -T_{u_i}.\Delta P_{m_i} - K_{t_i}(\frac{T_{g_i}}{r_i}\Delta P_{V_i} + \frac{\Delta\delta_i + \Delta\delta_{ref_i}}{r_i}) - \Delta E_{g_i}. \tag{A.2}$$

Eq. (46) remains unchanged and Eq. (47) can be rewritten as:

$$\begin{aligned}\Delta\dot{P}_{V_i} = {} & \frac{D_i.\Delta\delta_i + T_{u_i}.\Delta P_{m_i} + \frac{K_{t_i}}{r_i}(T_{g_i}\Delta P_{V_i} + \Delta\delta_i + \Delta\delta_{ref_i})}{M_i.T_{g_i}} \\ & \frac{-r_i.\Delta P_{V_i}}{T_{g_i}} + \frac{\Delta\omega_{ref_i}}{T_{g_i}} + \frac{\Delta E_{g_i}}{M_i.T_{g_i}}.\end{aligned} \tag{A.3}$$

Consequently, the local state variables are defined as: $x_{N_i} = \begin{bmatrix} \delta_i & P_{m_i} & P_{V_i} \end{bmatrix}^T$.

However, to develop local dynamics for all of the generator units in the region, one can combine Eqs. (46), (A.2), and (A.3), which leads to:

$$\Delta\dot{x}_{N_i} = A_{N_i}.\Delta x_{N_i} - c_{N_i}.\Delta E_{g_i} + b_{N1_i}.\Delta\delta_{ref_i} + b_{N2_i}.\Delta\omega_{ref_i}, \tag{A.4}$$

where c_{N_i} and A_{N_i} are obtained from Eqs. (49) and (50); therefore:

$$b_{N1_i} = \begin{bmatrix} \frac{-K_{t_i}}{M_i.r_i} & 0 & \frac{-K_{t_i}}{M_i.T_{g_i}.r_i} \end{bmatrix}^T \tag{A.5}$$

and

$$b_{N2_i} = \begin{bmatrix} 0 & 0 & \frac{1}{T_{g_i}} \end{bmatrix}^T \tag{A.6}$$

assuming that the governor controls are in a way that the closed-loop transient dynamics are fast relative to the updating of the reference values. Under this assumption, one can write $\dot{x} = 0$, $at\, kT_s$, $k = 0, 1, ..., ,$ i.e. the system can be settled to a steady-state for these discrete time instants kT_s. Let us first consider the local dynamic of each G–T–G set, derived in Eq. (A.4). The assumption of fast transient dynamics is yielded as:

$$0 = A_{N_i}.\Delta x_{N_i}[k] - c_{N_i}.\Delta E_{g_i}[k] + b_{N1_i}.\Delta\delta_{ref_i}[k] + b_{N2_i}.\Delta\omega_{ref_i}[k] \tag{A.7}$$

or

$$\Delta x_{N_i}[k] = A_{N_i}^{-1}c_{N_i}.\Delta E_{g_i}[k] - A_{N_i}^{-1}b_{N1_i}.\Delta\delta_{ref_i}[k] - A_{N_i}^{-1}b_{N2_i}.\Delta\omega_{ref_i}[k] \tag{A.8}$$

Since A_{N_i} is invertible, one now can easily control the output variables with input control signals $\Delta\delta_{ref_i}$ and $\Delta\omega_{ref_i}$.

B. Appendix: State space matrix

In this paper, the numerical state matrix A_N, the input matrix b, and the output matrix C_N of the proposed model are as follows:

$$C_N = \begin{bmatrix} 0.1000 & 0 & 0 \\ 0 & 0 & 0 \\ -0.4000 & 0 & 0 \\ 0 & 0.2000 & 0 \\ 0 & 0 & 0 \\ 0 & -0.8000 & 0 \\ 0 & 0 & 0.3333 \\ 0 & 0 & 0 \\ 0 & 0 & -1.3333 \end{bmatrix}, \quad b = \begin{bmatrix} 0 & 0 & 0 \\ 0 & 0 & 0 \\ 4 & 0 & 0 \\ 0 & 0 & 0 \\ 0 & 0 & 0 \\ 0 & 4 & 0 \\ 0 & 0 & 0 \\ 0 & 0 & 0 \\ 0 & 0 & 4 \end{bmatrix},$$

$$A_N = \begin{bmatrix} -0.0506 & -0.0200 & -0.0001 & 0 & 0 & 0 & 0 & 0 & 0 \\ 0 & -5.0000 & 0.5350 & 0 & 0 & 0 & 0 & 0 & 0 \\ -0.1977 & 0.0800 & -75.9994 & 0 & 0 & 0 & 0 & 0 & 0 \\ 0 & 0 & 0 & -0.0811 & -0.0400 & -0.0003 & 0 & 0 & 0 \\ 0 & 0 & 0 & 0 & -5.0000 & 0.5350 & 0 & 0 & 0 \\ 0 & 0 & 0 & -0.3155 & 0.1600 & -75.9989 & 0 & 0 & 0 \\ 0 & 0 & 0 & 0 & 0 & 0 & -0.1352 & -0.0667 & -0.0005 \\ 0 & 0 & 0 & 0 & 0 & 0 & 0 & -5.0000 & 0.5350 \\ 0 & 0 & 0 & 0 & 0 & 0 & -0.5258 & 0.2667 & -75.9981 \end{bmatrix}.$$

C. Appendix: Controllability and observability

A part of the Simulink block diagram in Figure 12 is shown here. Using MATLAB and Simulink, one is able to trace the observability and controllability of the problem. 'CTRB', computes the controllability matrix and 'CTRB(A,B)' returns the controllability matrix [B AB A∧2B ...].

'OBSV' computes the observability matrix and 'OBSV(A,C)' returns the observability matrix [C; CA; CA∧2 ...]. Furthermore, 'RANK(A)' provides an estimate of the number of linearly-independent rows or columns of matrix A.

The system is controllable if the controllability matrix has a full rank and the system is observable if the observability matrix has a full rank. Therefore, one may see the controllability and observability.

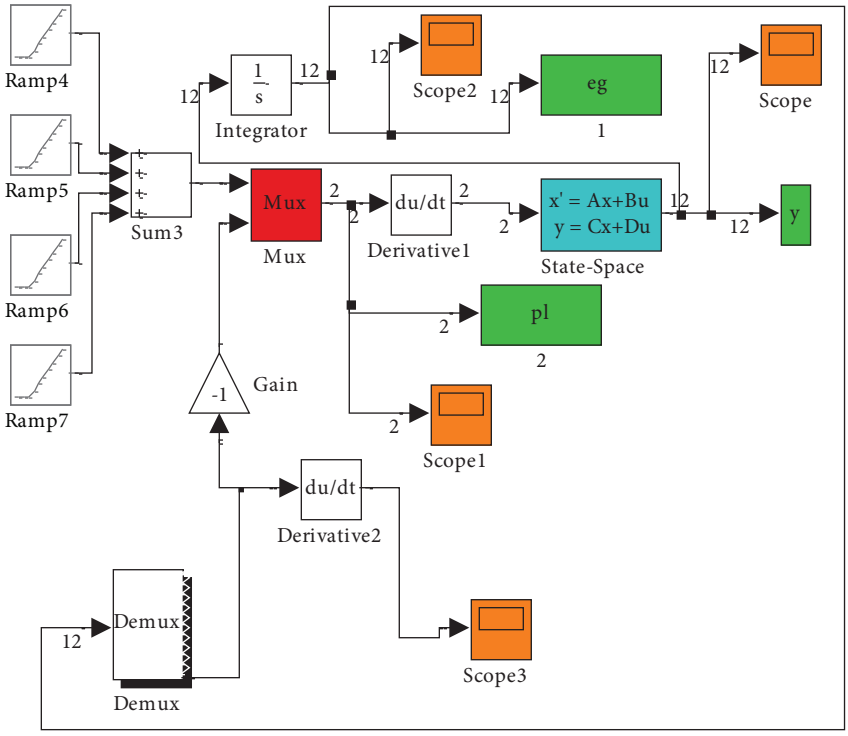

Figure 12. A part of the Simulink block diagram.

References

[1] T. Gómez, G. Rothwell, Electricity Economics Regulation and Deregulation, New York, Wiley, 2003.

[2] A.J. Wood, B.F. Wollenberg, Power Generation Operation and Control, New York, Wiley, 1996.

[3] E. Rakhshani, A. Sadeh, "Practical viewpoints on load frequency control problem in a deregulated power system", Energy Conversion and Management, Vol. 51, pp. 1148–1156, 2010.

[4] Y.M. Park, K.Y. Lee, "Optimal decentralized load frequency control", Electric Power Systems Research, Vol. 7, pp. 279–288, 1984.

[5] P.K. Ibraheem, D.P. Kothari, "Recent philosophies of automatic generation control strategies in power systems", IEEE Transactions on Power Systems, Vol. 20, pp. 346–357, 2005.

[6] H. Shayeghi, H.A. Shayanfar, A. Jalili, "Load frequency control strategies: a state-of-the-art survey for the researcher", Energy Conversion Management, Vol. 50, pp. 344–353, 2009.

[7] R.D. Christie, A. Bose, "Load frequency control issues in power system operations after deregulation", IEEE Transactions on Power Systems, Vol. 11, pp. 1191–1200, 1996.

[8] V. Donde, A. Pai, I.A. Hiskens, "Simulation and optimization in an AGC system after deregulation", IEEE Transactions on Power Systems, Vol. 16, pp. 481–489, 2001.

[9] K. Sedghisigarchi, A. Feliache, A. Davari, "Decentralized load frequency control in a deregulated environment using disturbance accommodation control theory", Proceedings of the 34th Southeastern Symposium in System Theory, pp. 302–306, 2002.

[10] D. Menniti, A. Pinnarelli, N. Scordino, "Using a FACTS device controlled by a decentralized control law to damp the transient frequency deviation in a deregulated electric power system", Electric Power System Research, Vol. 72, pp. 289–298, 2004.

[11] S.P. Ghoshal, "Multi area frequency and tie line power flow control with fuzzy logic based integral gain scheduling", Journal of Industrial Engineering, Vol. 84, pp. 135–41, 2003.

[12] T. Barjeev, S.C. Srivastava, "A fuzzy logic based load frequency controller in a competitive electricity environment", IEEE Power Engineering Society General Meeting, pp. 134–140, 2003.

[13] H. Bevrani, "A novel approach for power system load frequency controller design", IEEE/PES Transmission and Distribution Conference and Exhibition, pp. 184–190, 2002.

[14] H. Shayeghi, H.A. Shayanfar, A. Jalili, "Multi-stage fuzzy PID power system automatic generation controller in deregulated environments", Energy Conversion and Management, Vol. 47, pp. 2829–2838, 2006.

[15] A. Demiroren, H.L. Zeynelgil, "GA application to optimization of AGC in three area power system after deregulation", International Journal of Electrical Power and Energy Systems, Vol. 29, pp. 230–240, 2007.

[16] K.Y. Lim, Y. Wang, R. Zhou, "Robust decentralized load-frequency control of multi-area power systems", IEE Proceedings on Transmission and Distribution Part C, Vol. 143, pp. 377–386, 1996.

[17] H. Shayeghi, H.A. Shayanfar, "Decentralized robust AGC based on structured singular values", Journal of Electrical Engineering, Vol. 57, pp. 305–317, 2006.

[18] H. Bevrani, Y. Mitani, Tsuji K. "Robust decentralized AGC in a restructured power system", Energy Conversion Management, Vol. 45, pp. 2297–2312, 2004.

[19] H. Bevrani, Y. Mitani, K. Tsuji, H. Bevrani, "Bilateral based robust load frequency control", Energy Conversion Management, Vol. 46, pp. 1129–1136, 2005.

[20] H. Shayeghi, H.A. Shayanfar, "Design of decentralized robust LFC in a competitive electricity environment", Journal of Electrical Engineering, Vol. 56, pp. 225–236, 2005.

[21] H. Shayeghi, "A robust decentralized power system load frequency control", Journal of Electrical Engineering, Vol. 59, pp. 281–293, 2008.

[22] E.S. Ali, S.M. Abd-Elazim, "Bacteria foraging optimization algorithm based load frequency controller for interconnected power system", International Journal of Electrical Power and Energy Systems, Vol. 33, pp. 633–638, 2011.

[23] K.R. Sudha, R.V. Santhi, "Robust decentralized load frequency control of interconnected power system with generation rate constraint using type-2 fuzzy approach", International Journal of Electrical Power and Energy Systems, Vol. 33, pp. 699–707, 2011.

[24] M.T. Alrifai, M.F. Hassan, M. Zribi, "Decentralized load frequency controller for a multi-area interconnected power system", International Journal of Electrical Power and Energy Systems, Vol. 33, pp. 198–209, 2011.

[25] A. Yazdizadeh, M.H. Ramezani, E. Hamedrahmat, "Decentralized load frequency control using a new robust optimal MISO PID controller", International Journal of Electrical Power and Energy Systems, Vol. 35, pp. 57–65, 2012.

[26] W. Tan, H. Zhang, M. Yu, "Decentralized load frequency control in deregulated environments", International Journal of Electrical Power and Energy Systems, Vol. 33, pp. 1234–1241, 2012.

[27] H. Shayeghi, H.A. Shayanfar, O.P. Malik, "Robust decentralized neural networks based LFC in a deregulated power system", Electric Power System Research, Vol. 77, pp. 241–251, 2007.

[28] X.S. Liu, "Structural modeling and hierarchical control of large scale electric power systems", PhD Thesis, Department of Mechanical Engineering, MIT, USA, 1994.

[29] M.D. Ilic, X.S. Liu, "A modeling and control framework for operation large scale electric power systems under present and newly evolving competitive industry structures", International Journal of Mathematical Problems in Engineering, Vol. 1, pp. 317–340, 1996.

[30] M. Eidiani, "A reliable and efficient method for assessing voltage stability in transmission and distribution networks", International Journal of Electrical Power Energy Systems, Vol. 33, pp. 453–456, 2011.